The NMR-laser : a nonlinear solid state system showing chaos

Autor(en): **Brun, E. / Derighetti, B. / Holzner, R.**

Objekttyp: **Article**

Zeitschrift: **Helvetica Physica Acta**

Band (Jahr): **56 (1983)**

Heft 1-3

PDF erstellt am: **22.07.2024**

Persistenter Link: https://doi.org/10.5169/seals-115423

Helvetica Physica Acta,
Vol. 56 (1983) 825-836

0018-0238/83/010825-12$1.50+0.20/0

THE NMR-LASER - A NONLINEAR SOLID STATE SYSTEM SHOWING CHAOS*

E. Brun, B. Derighetti, R. Holzner and D. Meier
Physik-Institut, Universität Zürich, CH-8001 ZUERICH.

1. INTRODUCTION

The remarkable results on iterations of continuous maps of an interval into itself by J.M. Feigenbaum, J.P. Eckmann, S. Grossmann, and others [1] have stimulated experimentalists to search for pathways from simple to chaotic behavior of nonlinear physical many-body systems. For the most simple devices, such as driven nonlinear electronic oscillators, the existence of a Feigenbaum scenario within certain parameter ranges has been demonstrated convincingly [2]. There the approach to chaos goes over a set of period-doubling bifurcations with universal scaling properties. Physically more complex systems, such as Rayleigh-Bénard cells [3], chemical reactors [4], optically bistable devices [5], lasers [6] etc, yield experimental results which have to be interpreted with caution. Unknown noise sources, long-time drifts, slowing-down and hysteresis effects, a complex structure of the interlaced basins of attraction, and an extreme sensitivity on control and system parameters hamper the unambiguous determination of defined roads to chaotic behavior from the so far reported experimental material.

In this communication, we report novel experimental observations along the road to chaos of a tuned low-Q solid state spin-flip NMR laser which, according to our earlier work [7], should show the universal Feigenbaum scenario under certain conditions.

We have studied the nonlinear low-frequency response of the NMR laser activity to an external sinusoidal perturbation of one of its system parameters. Comparison of experimental results with computer solutions of an approximate theoretical model based on Bloch-type order parameter differential equations reflect instructively some of the difficulties an experimenter may encounter when he is out to detect unpaved physical roads to chaos.

2. THE RUBY RASER AND ITS MODELLING

A single ruby crystal ($Al_2O_3;Cr^{3+}$), onto which an rf-coil is wound, is cooled inside a microwave cavity to 1.6 K in a magnetic field B_0 of about 1.1 T. A 100 mW microwave generator is tuned to a selected ESR line of Cr^{3+} near 30 GHz, causing an enhancement of the nuclear magnetization $\underline{M}$ by means of dynamic nuclear polarization (DNP). Adjusting the DNP pump properly leads to a negative nuclear spin polarization (spin inversion). If now the coil is tuned with an external capacitor to one of the $\Delta m=\pm 1$ NMR transitions of the ^{27}Al nuclear spin system, spin energy is radiated coherently into the rf-coil, provided that $\underline{M}$ is pumped above a certain threshold. The coil provides the slaving feedback field $\bar{B}_1^r$ which causes the superfluorescent ordering of the precessing spins. The system then behaves laser-like. Thus we call it NMR laser or RASER (from radiowave amplification by stimulated emission of radiation).

*The work is supported in partial by a grant of the Swiss National Science Foundation.

We have shown [8] that a low-Q ruby raser may, to a good approximation, be treated as a homogeneous two-level system if only one NMR mode is excited. Then it can be modelled on time through generalized Bloch-type equations for its order parameters. If the raser is forced to purely absorptive behavior where the NMR frequency ω_0 coincides with the resonance frequency ω_L of the tuned coil and the raser frequency ω_R of the emitted radiowave (typically 12 MHz), we may neglect dispersion. Then we characterize the raser by three macroscopic order parameters only. They are the longitudinal magnetization M_z, the rotating magnetization M_v, and the rotating raser field B_1^r which is 90° out-of-phase with respect to M_v. Under certain conditions (low-Q case, weak raser activity, fast effective pump) we can simplify the general raser equations drastically [9]. For the (1/2, -1/2)NMR mode, for example, we obtain in the rotating frame approximation (in SI-units)

$$\frac{dM_v}{dt} = 9\gamma M_z B_1 - M_v/T_2 \qquad (1)$$

$$\frac{dM_z}{dt} = -\gamma M_v B_1 - (M_z - M_e)/T_e \qquad (2)$$

$$B_1^r = -\frac{1}{2}\mu_o \eta Q M_v \qquad (3)$$

with $B_1 = B_1^d + B_1^r$. B_1^d stands for an additional rf-field and may be a phase-locked external driving field, or an effective noise field, or a superposition of both. The term M_v/T_2 describes the dissipation of phase memory of the presessing spins. $(M_z - M_e)/T_e$ represents the DNP pumping mechanism with M_e the effective pumping magnetization and T_e the effective pumping time.

Since B_1^r can be eliminated adiabatically, we may describe the composite system: nuclear spins, electronic spins, DNP pump plus radiation field in a 2-d phase space by the nonlinear equations

$$\frac{dM_v}{dt} = (-\frac{9}{2}\mu_o \eta Q \gamma M_v + 9\gamma B_1^d) M_z - M_v/T_2 \qquad (4)$$

$$\frac{dM_z}{dt} = (\frac{1}{2}\mu_o \eta Q \gamma M_v - \gamma B_1^d) M_v - (M_z - M_e)/T_e \; . \qquad (5)$$

These are our raser equations on which our analysis is based. Typical system parameters are the filling factor $\eta \tilde{=} 0.5$, the dephasing time $T_2 \tilde{=} 30\mu s$, $T_e = 0.1s$, $M_e = -1.6$ A/m, the quality factor of the coil $Q = 100$, $B_1^d \simeq 10^{-10}$ T. γ is the gyromagnetic ratio of ^{27}Al. The numerical factors are spin factors stemming from the spin-5/2 of ^{27}Al and its fictitious spin 1/2 (two-level) description. To demonstrate the reliability of the model we compare in Fig. 1 the transient behavior of the raser with computer solutions of (4) and (5). The top picture shows the observed envelope of the raser output after the LC-circuit has been tuned to ω_0 at $t = 0$. The output voltage in function of time is directly measured at the coil and stored on an oscilloscope or in a digital transient recorder. After tuning, a delayed giant pulse (clipped by a factor of 10) appears. Then after a dead time of approx. 0.15s follows a spiking behavior which is damped out to the steady raser activity. The two graphs below represent the corresponding computer solutions. The curves depict $M_v(t)$ and

$M_Z(t)$. The raser output is proportional to M_V. M_Z cannot be measured directly. The result that a perfectly tuned low-Q raser (or laser!) may be modelled onto trajectories in a 2-d phase space (M_V, M_Z) is rather surprising. However, this has been tested for driven NMR systems also where bistability, pseudo-bistability and steady spiking behavior have been found [7].

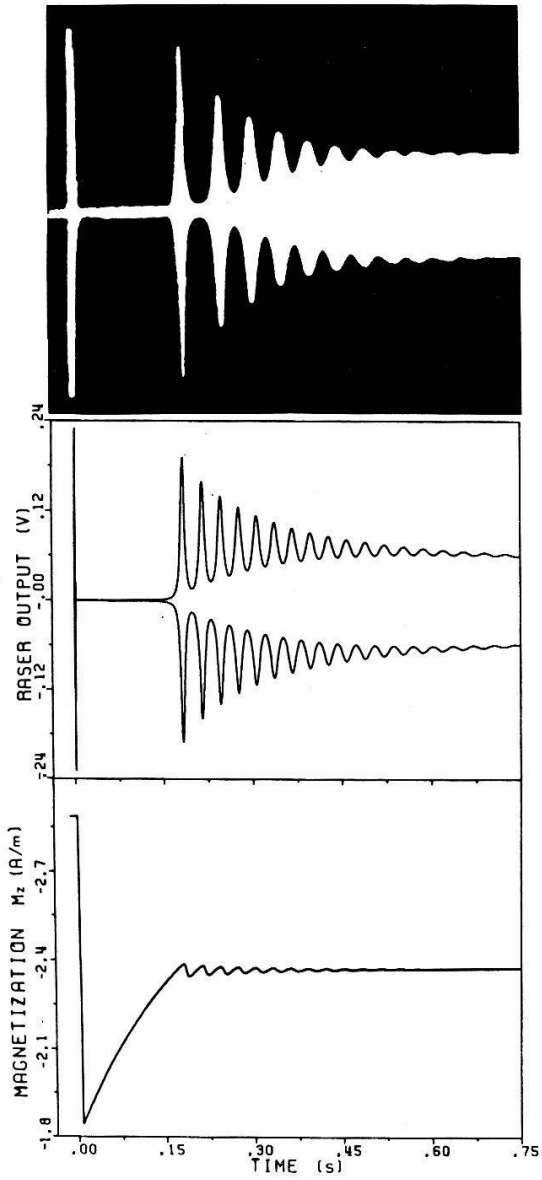

Fig. 1. Raser transients after tuning (Q-switching)

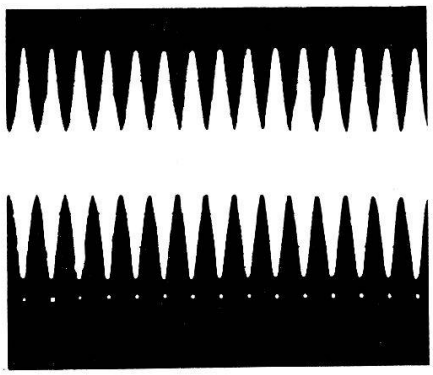

Fig. 2. Modulated raser output due to forced parameter modulation e.g. of Q, M_e, B_1^d or T_2. The time interval between equal time markers (dots) is 0.03s.

3. RASER MODULATION

The so far discussed system is effectively restricted to a 2-d phase space. The solutions of the nonlinear equations of motion behave regularly in time, and one finds only simple pictorial representations for the orbits in phase space. To augment its dimension, where one expects to detect basins of complex behavior, we let an externally controlled system parameter vary in time. One has the choice to modulate either Q, M_e or B_1^d. By applying a weak time-varying field gradient to B_0, we can effectively modulate T_2, even. We have modulated, for example, the pumping magnetization sinusoidally with a frequency Ω close to

the eigenfrequency of the linearized raser equation near its steady state solutions. Experimentally Ω can be estimated from the observed response of Fig. 1. A modulation of the raser output is shown in Fig. 2. A typical value for $f = \Omega/2\pi$ is 30 Hz. If F is the modulation strength, the raser may now be modelled by

$$\frac{dM_v}{dt} = (-\frac{9}{2}\mu_o\eta Q\gamma M_v + 9\gamma B_1^d) M_z - M_v/T_2 \qquad (6)$$

$$\frac{dM_z}{dt} = (\frac{1}{2}\mu_o\eta Q\gamma M_v - \gamma B_1^d) M_v - (M_z - M_e(1-F \sin \Omega t))/T_e . \qquad (7)$$

4. SUBHARMONICS AND CHAOS: RASER EXPERIMENTS

With the periodic low-frequency drive we add two control parameters to our system, the strength F of the drive and its natural period $T = 2\pi/\Omega$ which we call period-1. For F-values below a certain threshold F_1 the system is attracted towards a stable limit-cycle of period-1. Increasing the control parameter then leads usually to a series of bifurcations at F_n, n = 1, 2, 3... where attracting limit-cycles of period-2^n are born. In Fig. 3. we show the results of an experimental attempt to observe such a sequence of bifurcations which ends in a chaotic state. Extreme care is necessary to reproduce the depicted asymptotic stable limit-cycle behavior of defined period-2^n. Unidentified noise sources lead to spurious spectral components which already show up in the phase-space portraits and the power spectra of low-order limit-cycles. These effects often lead to a truncation of an expected bifurcation sequence. Any attempt to estimate universal constants from such data is fortuitous.

In our search for a Feigenbaum scenario we have observed a complex structure of the various basins of attraction. We have found many discontinuous jumps from one particular limit-cycle to another. For example, from a limit-cycle of period-3 (Fig. 4) to one of period-2 and from limit-cycles of period-N directly to chaos. Transitions of this sort are reminescent of a first-order phase transition and are accompanied by strong hysteresis effects. They are highly sensitive to noise and slow drifts. We have further found chaotic regions where the spectra vary intermittently in time between phases of weakly noisy quasi-periodic behavior and phases with strong broadband noise.

In addition, we have often detected so-called breathing modes where a limit-cycle is low-frequency modulated which leads to an oscillatory behavior. This effect is most commonly found in higher limit-cycles, but it has also been observed for a period-2 cycle where such a breather seems to be extremely stable. We believe that there is a close correspondence to similar observations as reported by Giglio et al. [3].

To illustrate some of the complexity of the modulated raser response, we show in Fig. 5 the raser amplitude in function of the drive frequency $f=\Omega/2\pi$ for different fixed modulation strengths F. For small F-values (in relative units) we have obtained the well-known nonlinear response curve with fold-over and switching properties. The system remains for all values of f in a limit-cycle of period-1. For F > 200, the response curve becomes multi-peaked with strong sensitivity to f. This is due to chaotic behavior for example. The high jumps are usually connected with the mentioned discontinuous transitions between different basins of attraction. Figure 6 shows the hysteresis loop for

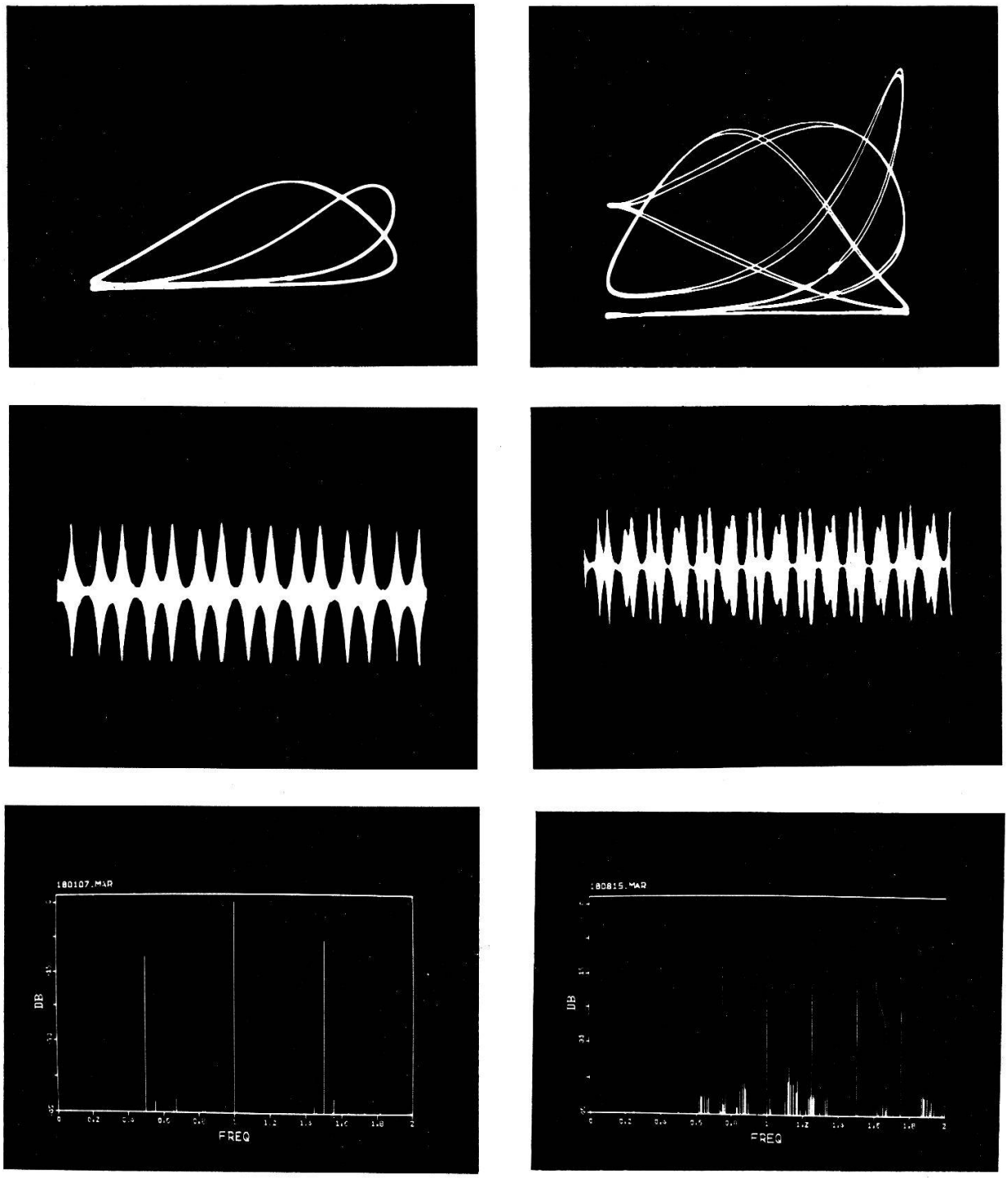

Fig. 3a. Experimental phase-space portraits, time response, and power spectra of a modulated raser in a limit-cycle behavior of period-2 and 4 with erratic noise. The portraits depict the raser output vs. modulator signal.

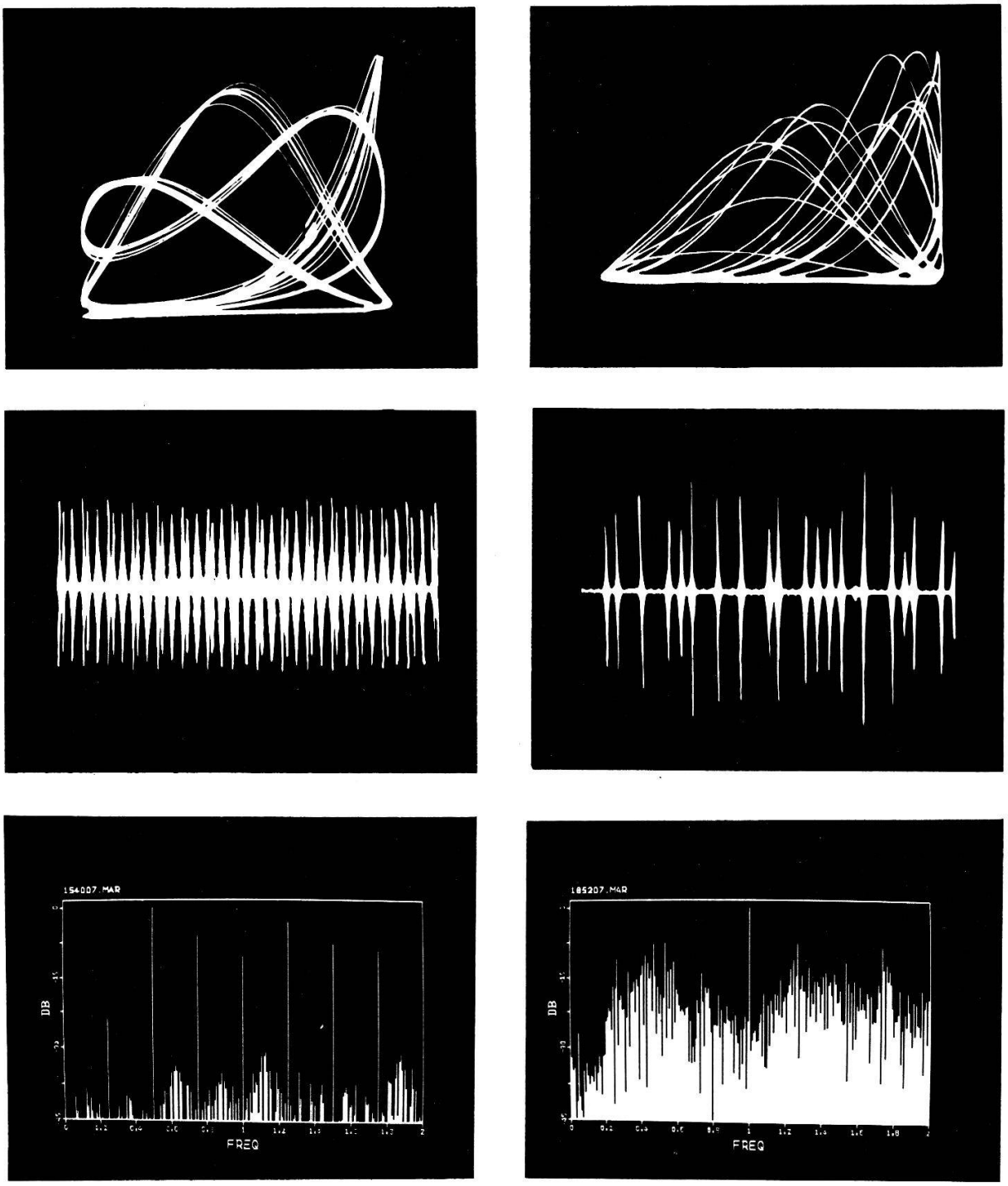

Fig. 3b. Experimental phase-space portraits, time response, and power spectra of a modulated raser in a weakly noisy period-8 limit-cycle and in a chaotic state.

the period-1 response which is reminescent to NMR bistability [7], here in the low-frequency response, there in the rf-response.

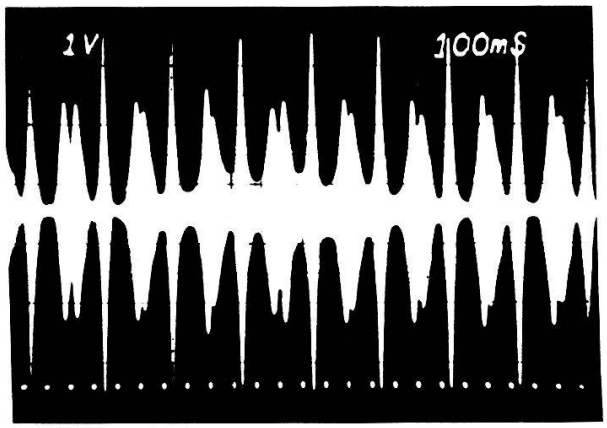

Fig. 4. Predominately a period-3 limit-cycle behavior of the raser. The dots are markers of period-1.

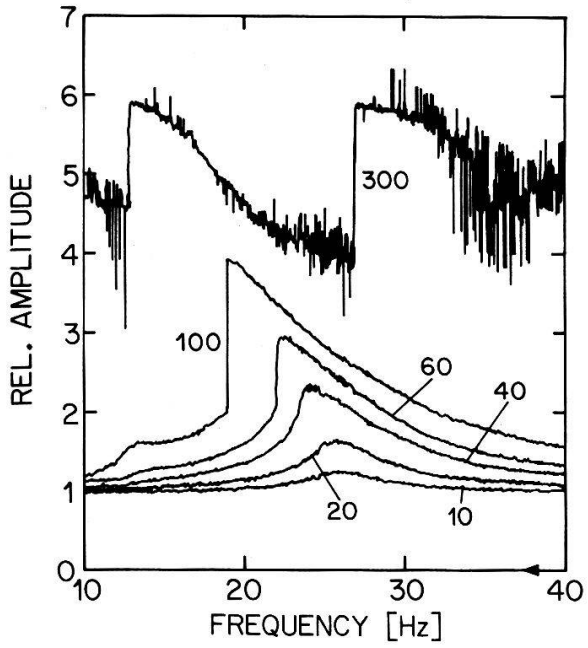

Fig.5. Experimental low-frequency response curve of a modulated raser in function of the drive frequency f for different values of the modulation strength F.

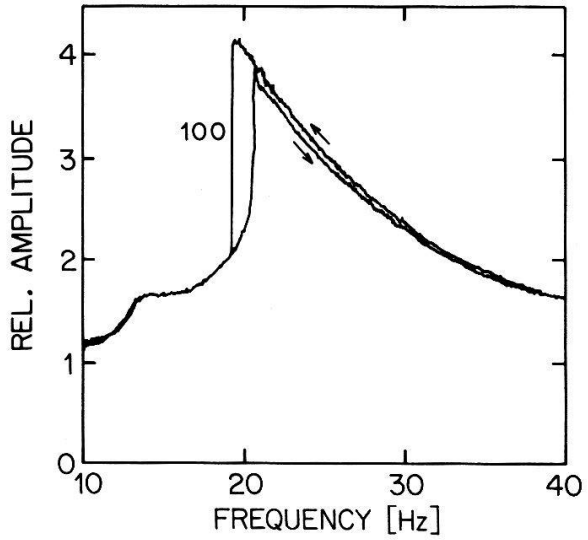

Fig. 6. Hysteresis in the low-frequency response of a modulated raser.

5. SUBHARMONICS AND CHAOS: COMPUTER EXPERIMENTS

In order to model some of our experiments we have looked for numerical solutions of (6) and (7). We present selected results which we consider as representative. The assumed system parameters are close to the actual physical values, e.g. Q = 100, $B_1^d = -10^{-10}$ T, $M_e = -1.6$ A/m, $T_2 = 3\times10^{-5}$s, $T_e = 0.1$s, $\Omega = 280s^{-1}$, F has been varied between 0 and 0.3.

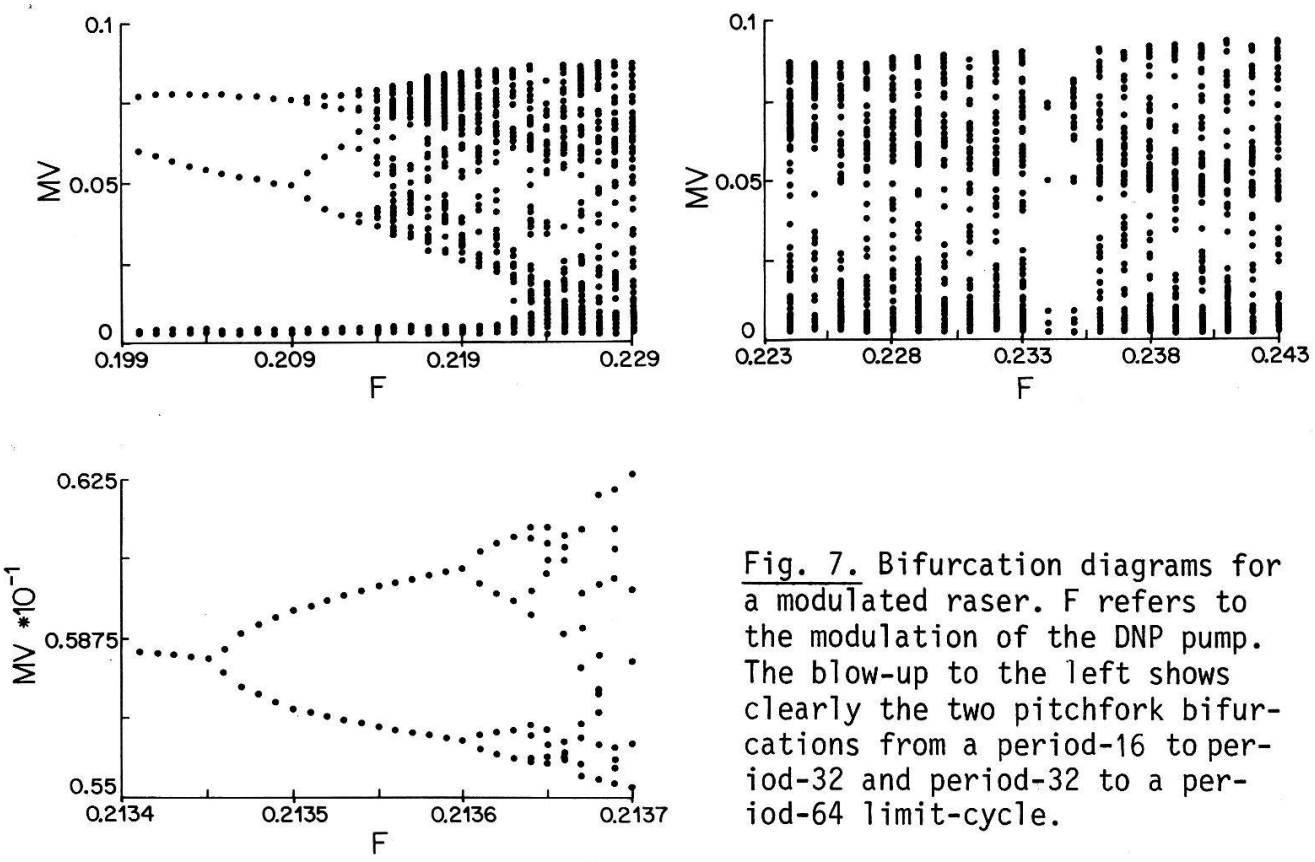

Fig. 7. Bifurcation diagrams for a modulated raser. F refers to the modulation of the DNP pump. The blow-up to the left shows clearly the two pitchfork bifurcations from a period-16 to period-32 and period-32 to a period-64 limit-cycle.

Figure 7 shows three bifurcation diagrams for F between 0.2 and 0.245. For each value of F 128 dots (one dot per period-1) are plotted which represent the asymptotic solution $M_v(t)$ of (6) and (7) at discrete times. We see clearly a sequence of bifurcations with period-doubling which leads to noisy bands (with an inverse cascade of period-doubling bifurcations which are not evident in the plot), a wide region with broadband noise and with a period-5 window near F=0.234. From blow-ups, as shown in Fig. 7 (in the last graph), one may determine the series F_n of bifurcations with period-doubling by 2^n, n = 1, 2, 3, 4... which converge to F_c. With our moderate resolution in the F-scale we have obtained the values $F_1=0.159000$, $F_2=0.196830$, $F_3=0.209650$, $F_4=0.212785$, $F_5=0.213445$, $F_6=0.213595$, $F_7=0.213625$ from which one finds the series of convergence rates $\Delta_1=2.95$, $\Delta_2=4.09$, $\Delta_3=4.75$, $\Delta_4=4.40$, $\Delta_5=5.00$ which have to be compared with the Feigenbaum limit $\Delta_\infty=4.6692016...$ Similar results have been found with other system parameters and for sequences in different windows inside the chaotic bands.

The bifurcation diagrams in Fig. 8 illustrate a different asymptotic behavior of the model system within the same range of the control parameter F as in Fig. 7. It is the outcome of different choice of initial conditions. With a few percent change in the initial conditions the system is attracted

towards a stable period-3 cycle e.g. for F=0.215. Increasing F does not lead to bifurcations. Slightly below F=0.2336 a jump to chaotic behavior results. Further increasing F brings the system after a narrow chaotic region into a period-5 window, followed by a sequence of bifurcations to limit-cycles of period-$5x2^n$. The chaotic region and the period-5 window of Fig. 8 are identical to the ones of Fig. 7.

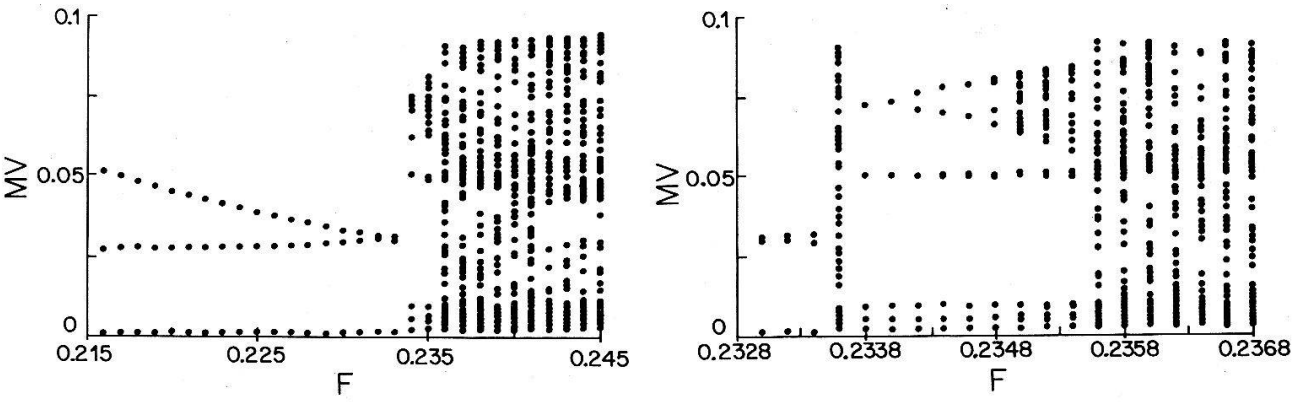

Fig. 8. Bifurcation diagrams for a modulated raser starting in period-3 limit-cycle (F = 0.215).

Figure 9 shows what happens when F is stepwise lowered. Starting in the period-3 cycle at F=0.2005 leads to an irreversible jump to period-2 cycle near F=0.1900. However, if we start in the noisy region at F=0.225, the system follows the route of Fig. 7 in the reverse sense. Hence, this route to and from the chaos is reversible.

Figure 10 depicts phase-space and time behavior together with Fourier power spectra of the period-8 cycle at F=0.212 and of the noisy band at F=0.222. From Fourier spectra of low-order period-2^n cycles we have found that the power per doubling goes down by about 19 dB.

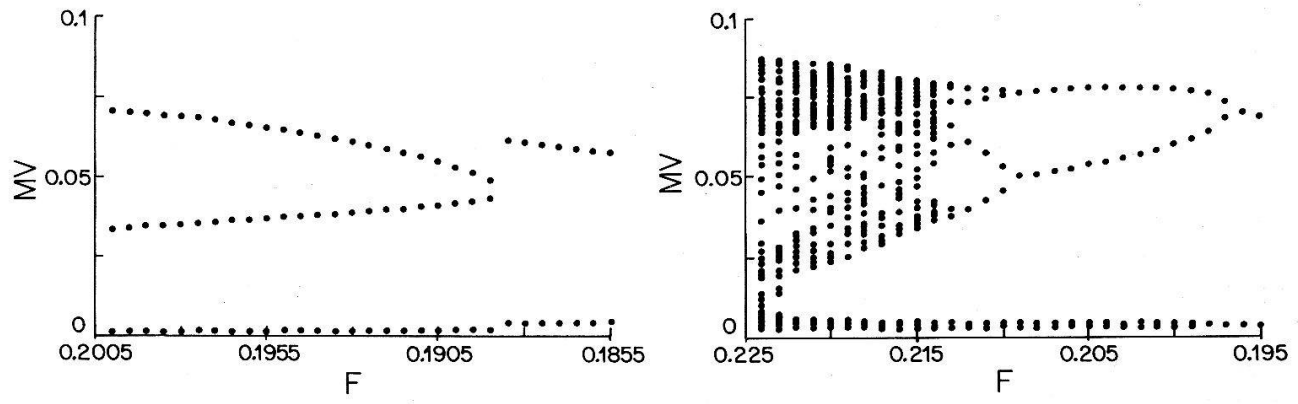

Fig. 9. Bifurcation diagrams of a modulated raser showing an irreversible transition (3.2) and a reversible path from and to the chaos.

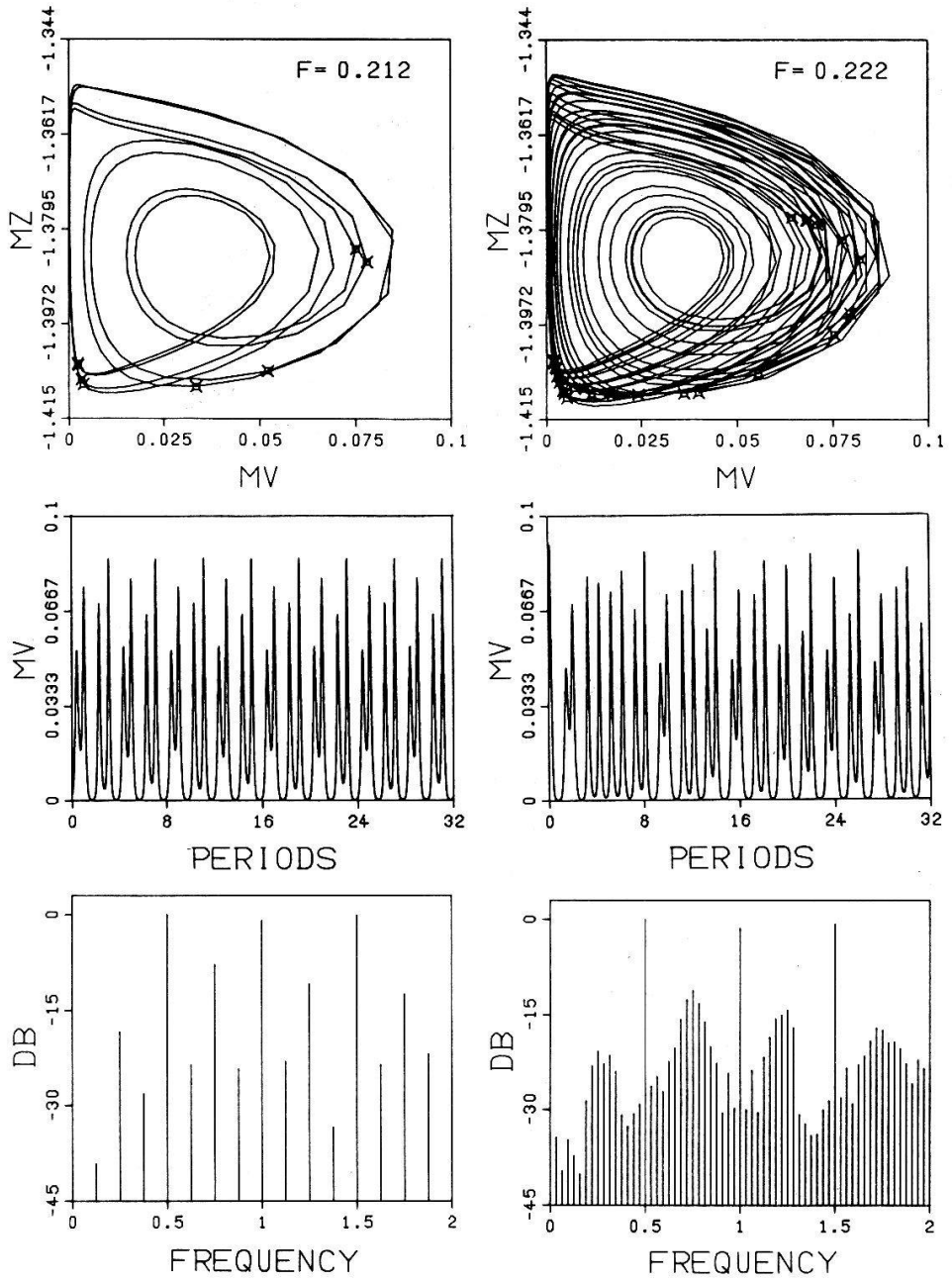

Fig. 10. Phase space portraits (M_V, M_Z), time behavior $M_V(t)$ and Fourier power spectra in an asymptotic periodic and nonperiodic state.

Figure 11 illustrates the dynamics of the irreversible transition from the period-3 to the period-2 cycle near F=0.1886. The given phase-space portraits are taken at various consecutive times, starting from a nonequilibrium initial state. The 1st portrait shows a transient which seems to lead to the stable period-3 cycle of the 2nd portrait. However, this is an illusion. As time goes on, slow changes become manifest which can be recognized as weak nonperiodicities (smeared out time-1 markers) in the 3rd and 4th portrait after a long waiting time between the 2nd and 3rd portrait. Then the situation changes drastically. A wild transient builds up (5th portrait) which ends, after a short transient time, in the stable period-2 cycle. In Fig. 12 we give the time behaviour which corresponds to the 3rd, 5th and 6th portrait. These graphs clearly show the fast

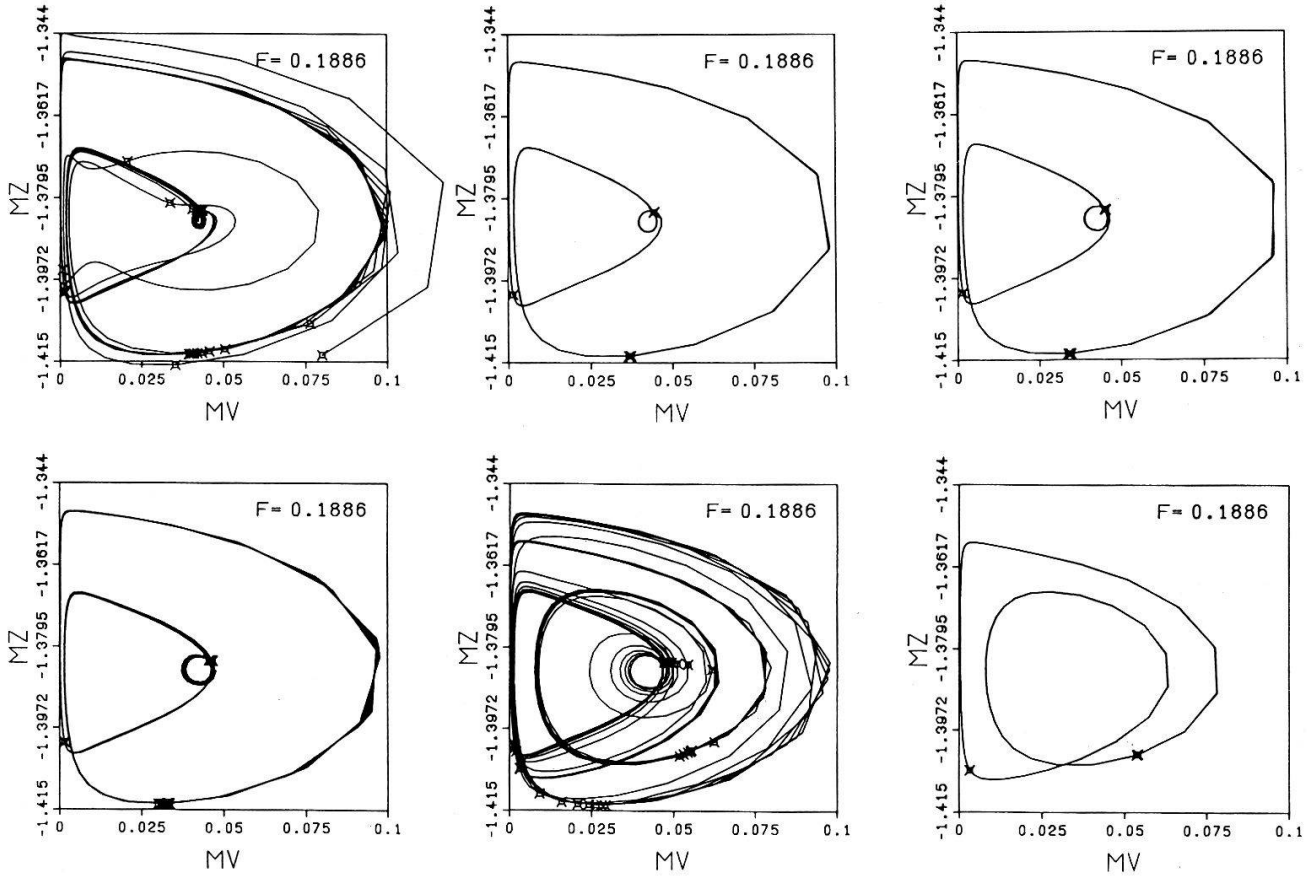

Fig. 11. Sequence of consecutive phase space portraits (32 natural time-1 units)

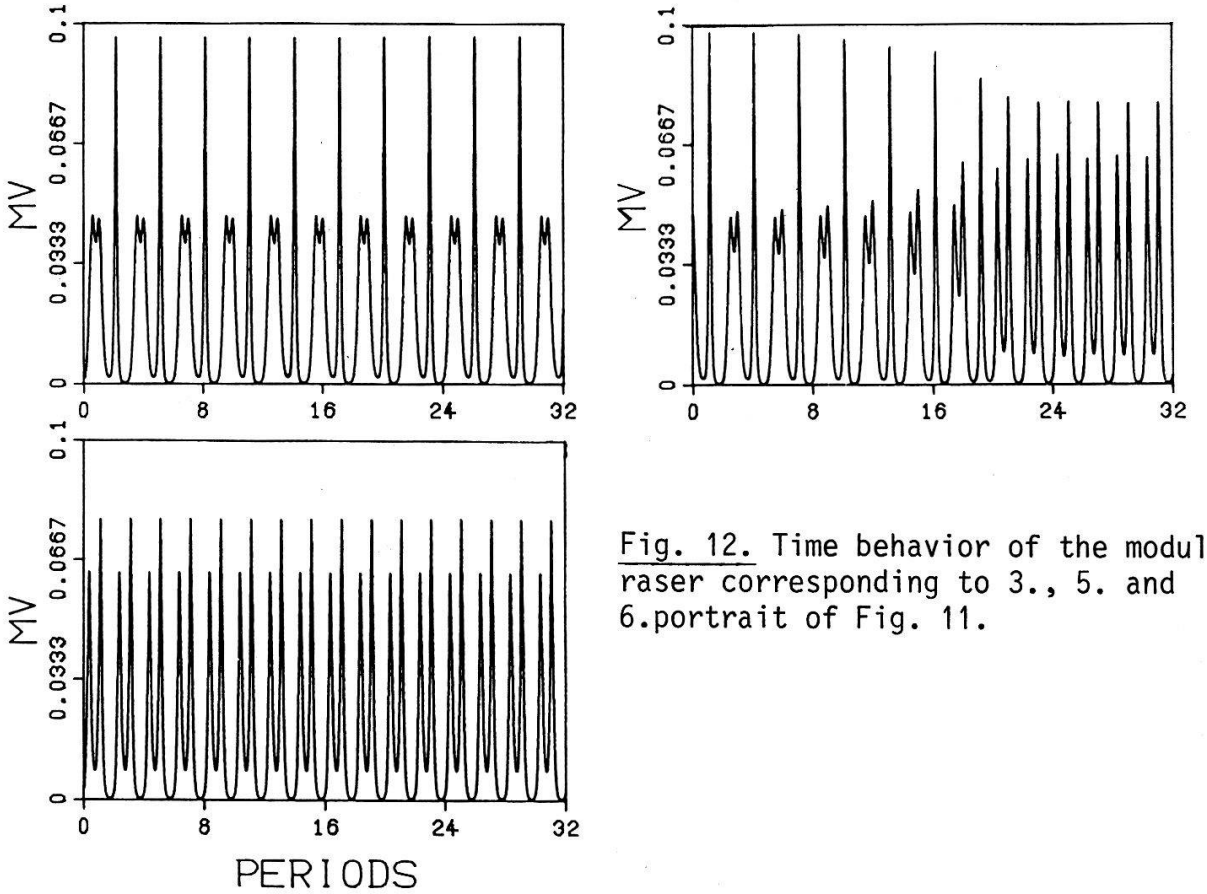

Fig. 12. Time behavior of the modulated raser corresponding to 3., 5. and 6.portrait of Fig. 11.

nonperiodic phase when the system jumps from one limit-cycle to another after a phase of extremely slow dynamics. We have found that the time spent in the phase where slowing-down occurs can be many orders of magnitude longer than the longest time constant of the system. This fact should not be overlooked when experiments and calculations are performed on limit-cycle behavior, otherwise premature conclusions may lead to erroneous interpretations.

6. CONCLUDING REMARKS

From the bulk of our experimental data and model calculations we may draw the conclusion that a Feigenbaum scenario indeed exists in laser-type devices. However, to get into the realm of its attractor requires carefully chosen initial conditions within small ranges in parameter space. Further, in order to remain there and be sure to have reached asymptotic behavior, extreme conditions have to be met, not only with respect to noise but also to the long-time stability, in particular. It seems that experimenters (including ourselves) have not reached the goal yet where realiable quantitative tests of limiting values of convergence rates and other universal scaling properties of nonlinear systems but the simplest can be made.

REFERENCES

[1] M.J.Feigenbaum, J.Stat.Phys.19,25(1978) and J.Stat.Phys.21,669(1979); J.P.Eckmann, Rev.Mod.Phys.53,643(1981); S.Grossmann, S.Thomae, Z.Naturforsch.32a,1353(1977); E.Ott, Rev.Mod.Phys.53,655(1981).

[2] Y.Ueda, J.Stat.Phys.20,1817(1979); P.S.Linsay, Phys.Rev.Lett.47,1349 (1981); J.Testa, J.Pérez, and C.Jeffries, Phys.Rev.Lett.48,714(1982); R.W.Rollins and E.R.Hunt, Phys.Rev.Lett.49,1295(1982).

[3] J.Maurer and A.Libchaber, J.Phys.Lett.(Paris)41,L515(1980); A.Libchaber and J.Maurer, J.Phys.Colloq.(Paris)41,C3-51(1980); M.Giglio, S.Musazzi, and U.Perini, Phys.Rev.Lett.47,243(1981); and in Evolution of Order and Chaos, Springer Series in Synergetics 17,174(1982).

[4] R.H.Simoyi, A.Wolf, and H.L.Swinney, Phys.Rev.Lett.49,245(1982).

[5] H.M.Gibbs, F.A.Hopf, D.L.Kaplan, and R.L.Shoemaker, Phys.Rev.Lett.46,474 (1981); F.A.Hopf, D.L.Kaplan, H.M.Gibbs, and R.L.Shoemaker, Phys.Rev.A25, 2172(1982); H.Nakatsuka, S.Asaka, H.Itoh, K.Ikeda, and M.Matsuoka, Phys. Rev.Lett.50,109(1983).

[6] F.T.Arecchi, R.Meucci, G.Puccioni, and J.Tredicce, Phys.Rev.Lett.49,1217 (1982).

[7] D.Meier, R.Holzner, B.Derighetti, and E.Brun, in Evolution of Order and Chaos, Springer Series in Synergetics 17,146(1982).

[8] P.Bösiger, E.Brun, and D.Meier, Phys.Rev.Lett.38,602(1977); and in Phys. Rev.A18,671(1978).

[9] P.Bösiger, E.Brun, and D.Meier, Phys.Rev.A20,1073(1979).